Materials Science and Engineering C 79 (2017) 15–22

Contents lists available at ScienceDirect

Materials Science and Engineering C

journal homepage: www.elsevier.com/locate/msec

Biomimetic electrospun scaffolds from main extracellular matrix components for skin tissue engineering application – The role of chondroitin sulfate and sulfated hyaluronan

Sirsendu Bhowmick [a,c], Sandra Rother [a], Heike Zimmermann [a], Poh S. Lee [a], Stephanie Moeller [b], Matthias Schnabelrauch [b], Veena Koul [c], Rainer Jordan [d], Vera Hintze [a], Dieter Scharnweber [a,*]

[a] Max Bergmann Center of Biomaterials, Technische Universität Dresden, Budapester Straße 27, 01069 Dresden, Germany
[b] Biomaterials Department, INNOVENT e.V., Prüssingstraße 27B, 07745 Jena, Germany
[c] Centre for Biomedical Engineering, Indian Institute of Technology Delhi, Hauz Khas, 110016 New Delhi, India
[d] Chair of Macromolecular Chemistry, Department of Chemistry and Food Chemistry, School of Science, TU Dresden, Mommsenstraße 4, 01069 Dresden, Germany

ARTICLE INFO

Article history:
Received 31 March 2017
Received in revised form 24 April 2017
Accepted 4 May 2017
Available online 4 May 2017

Keywords:
Sulfated glycosaminoglycans
Electrospun nanofibrous scaffolds
Cellular adhesion and proliferation

ABSTRACT

Incorporation of bioactive components like glycosaminoglycans (GAGs) into tissue engineering scaffolds, is a promising approach towards developing new generation functional biomaterial. Here, we have designed electrospun nanofibrous scaffolds made of gelatin and different concentrations of chemically sulfated or non-sulfated hyaluronan (sHA or HA) and chondroitin sulfate (CS). Evenly distributed fiber morphology was observed with no differences between varying concentrations and types of GAGs. *In vitro* release kinetics revealed that GAGs release is driven by diffusion. The effects of these scaffolds were analyzed on human keratinocyte (HaCaT), fibroblast (Hs27) and mesenchymal stem cells (hMSCs) adhesion and proliferation. A significant increase in cell number (~5 fold) was observed when cultivating all three cell types alone on scaffolds containing sHA and CS. These findings suggest that sulfated GAG-containing electrospun nanofibrous scaffolds might be beneficial for the development of effective skin tissue engineered constructs by stimulating cellular performance and therefore accelerate epidermal-dermal regeneration processes.

1. Introduction

The development of artificial scaffolds has long been achieved, while those for specific applications and functions, *e.g.* reducing the infections and scarring are now in focus. Tissue-engineered skin replacement can be used for a wide range of therapeutical application *viz.*, (a) acute, chronic and trauma skin wounds/ulcer treatment, (b) diabetic ulcer and venous stasis and (c) surgical injury and abrasion. The major goal of skin substitutes is not only to functionally support the wounded tissue and promote healing but also to be straightforwardly applicable under emergency/clinical circumstances [1].

The extracellular matrix (ECM) is a principal constituent of the intracellular-microenvironment, playing a pivotal role of maintaining and regulating tissue function [2,3]. Thus, incorporating essential components of ECM in biologically functional scaffolds to mimic this microenvironment is an efficient approach to control cellular proliferation process in tissue regeneration [3,4]. Except for hyaluronan (HA), the native GAGs are always present in sulfated form [5]. GAGs play a crucial role in different stages of skin tissue regeneration and maturation, being an important component of its ECM [6] and able to bind a number of proteins including several chemokines and growth factors [1]. The carbohydrate backbone of GAGs as well as the position and number of sulfate groups within the polymer chain plays an important role on these GAG-protein interactions [7]. Incorporation of HA/chondroitin sulfate (CS) combination into tissue engineered scaffold is widely reported in literature [8–13]. Fabrication of electrospun based scaffold for tissue engineering application is well known for its native tissue mimicking properties [14–19]. Recently, we have reported that sericin loaded cationic gelatin composite electrospun nanofibrous scaffold (cationic gelatin/HA/CS) stimulates epithelial differentiation of hMSCs in keratinocyte-hMSC co-culture model in terms of various epithelial markers (pan-cytokeratin, keratin 14 and p63) [20]. Previously, our group have also explored the interactions of native as well as chemically modified GAGs with different sugar backbones and variable types of functional groups for their binding affinities to growth factors relevant in skin and bone healing. These studies demonstrated that chemically modified hyaluronan derivatives with high sulfation degree (sHA, average sulfation degree per repeating-disaccharide unit ((DS_S) ~3) displayed strong interaction with TGF-β1, BMP-2 and -4 in 2D cell culture [7,21] and can be considered a promising support for regenerative medicine for epithelial damage treatments. Other research

* Corresponding author at: Max Bergmann Center of Biomaterials, Institute of Materials Science, Technische Universität Dresden, 01069 Dresden, Germany.
E-mail address: Dieter.Scharnweber@tu-dresden.de (D. Scharnweber).

http://dx.doi.org/10.1016/j.msec.2017.05.005
0928-4931/

group like Van der Smissen et al. demonstrated that degree of sulfation of GAGs influences the initial cellular attachment of human dermal fibroblasts (hDF) on collagen I/sulfated hyaluronan scaffolds after 24 h [1]. Similarly Salbach-Hirsch et al. showed that the sulfated HA significantly control osteoclastogenesis process significantly by interfering the formation of RANKL/OPG complex [22].

Against these background chemically sulfated sHA and naturally sulfated CS as functional constituents and gelatin as a cellular substrate were used to fabricate biomimetic nanofibrous 3D scaffold platform, which could act as a skin wound dressing, mimicking the extracellular microenvironment and thereby promoting wound healing process.

2. Materials and methods

2.1. Materials

2,2,2-Trifluoroethanol (TFE), mitomycin C and gelatin from porcine skin gel strength 300, Type A were obtained from Sigma-Aldrich, USA. Chondroitin sulfate from porcine trachea (a combination of 30% chondroitin-6-sulfate and 70% chondroitin-4-sulfate, sulfation degree of 0.9, Mw = 20,000 g/mol) was acquired from Kraeber (Ellerbek, Germany). Hyaluronan (Mw $1.1 \cdot 10^6$ g/mol; polydispersity 4.8) from *Streptococcus* was bought from Aqua Biochem (Dessau, Germany).

2.2. Synthesis of low molecular weight HA and sulfated HA

Sulfated HA and low molecular weight HA was synthesized and evaluated as described previously [21,23,24]. Concisely, the tetrabutylammonium salt of hyaluronan (TeBA-HA) was used as reactant for the sulfation reaction. The procedure is described as follows:

General procedure: 2.0 g (4.98 mmol) of HA was dissolved in 400 ml of double distilled water by stirring continuously for overnight at room temperature. Afterwards, 20 g of Dowex WX 8 ion exchanger (tetrabutylammonium-form) was mixed with the solution and kept overnight in continuous stirring. The final solution was filtered and lyophilized overnight and kept in vacuum oven at 40 °C for drying. Yield = 90%.

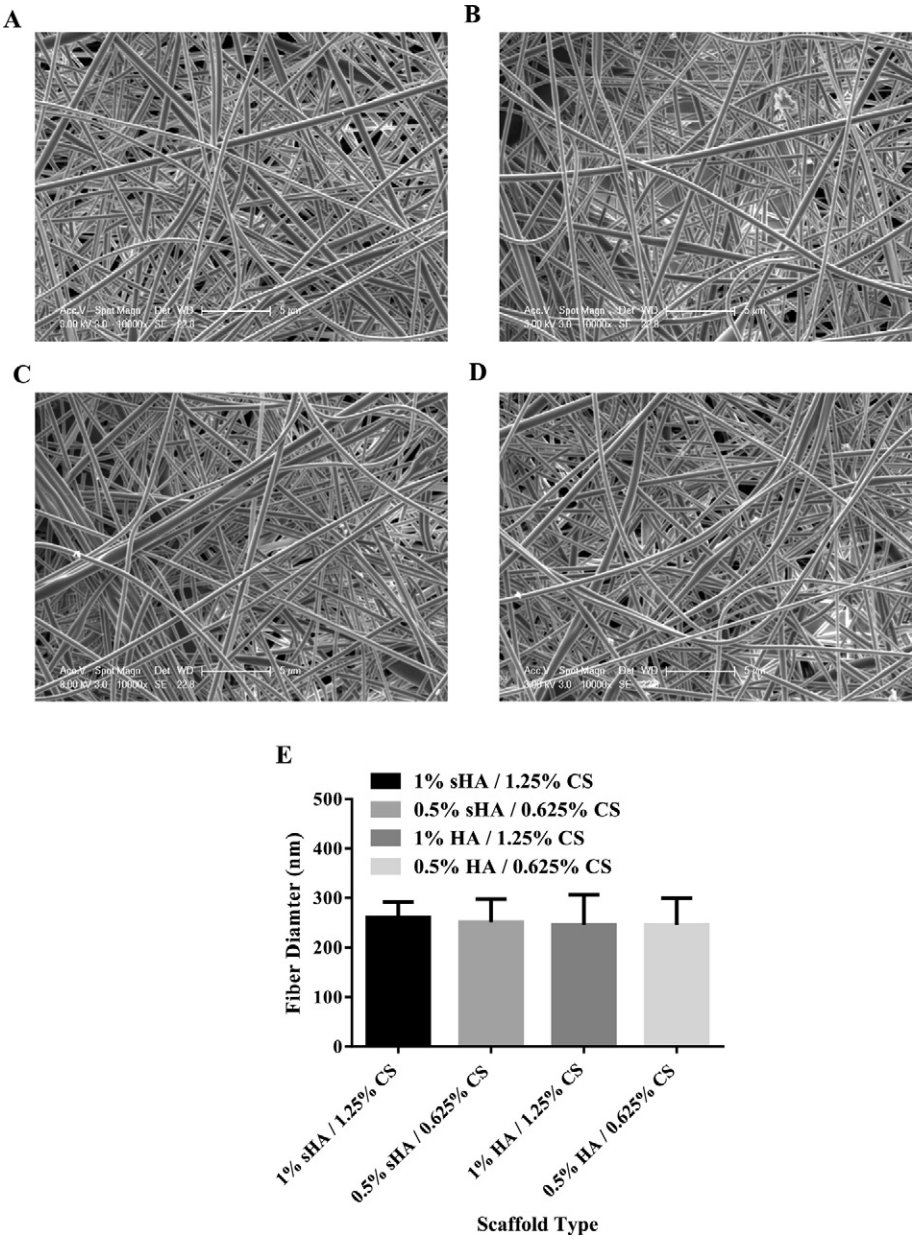

Fig. 1. Characterization of electrospun scaffolds; SEM image of electrospun scaffold (A) 1% sHA/1.25% CS, (B) 0.5% sHA/0.625% CS, (C) 1% HA/1.25% CS and, (D) 0.5% HA/0.625% CS and (E) Fiber diameter distribution of the scaffolds in SEM image.

High-sulfated HA (*sHA* 3.0): 2.0 g of TeBA-HA (3.22 mmol) was suspended in 400 ml of DMF at room temperature under argon gas environment followed by adding of SO_3–DMF complex (9.9 g, 64.4 mmol) dissolved in 40 ml dimethylformamide (polymer/SO_3 1:20). The resulting solution was continuously stirred for 1 h at room temperature. Yield = 70% (associated with HA-Na).

2.3. Electrospinning of gelatin, sulfated hyaluronan and chondroitin sulfate

10% (w/v) gelatin, 1–0.5% (w/v) sHA/1–0.5% (w/v) non-sulfated HA and 1.25–0.625% (w/v) CS were dissolved in 50% (v/v) 2,2,2-Trifluoroethanol (TFE). Under temperature (30 °C) and controlled relative humidity (45% RH), the electrospinning was performed with a flow rate, voltage and collector distance of 0.75 ml/h, 20 kV and 13 cm, respectively. Electrospinning fibrous scaffold with 10% (w/v) gelatin, 1–0.5% (w/v) non-sulfated HA and 1.25–0.625% (w/v) CS was prepared for comparison studies. Glutaraldehyde vapor (GTA) was used to crosslink the scaffold (30 min incubation) [25]. Then the fibrous scaffolds were kept in a vacuum oven for overnight and kept at 4 °C in a desiccator for storage.

2.4. Characterization of scaffolds

The surface property of scaffold was captured in XL30ESEM-FEG, Scanning Electron Microscope (FEI) after carbon coating in Polaron sputter coating unit. Five SEM images were considered to determine the mean fiber diameter (Photoshop 8.0). As a minimum of 25 fibers and 100 sections were selected arbitrarily for the evaluation [26,27].

The scaffolds were stained with Sirius red [28,29] and Toluidin blue [30] to observe the distribution of gelatin and GAGs, respectively.

2.5. In vitro release behavior of GAGs

The release of sulfated GAGs from the electrospun nanofibrous scaffold was studied by dimethyl methylene blue (DMMB) assay [31] in pH 7.5 phosphate buffer. The scaffold was submerged in 1 ml phosphate buffer and kept inside a 37 °C incubator shaker. Samples were collected after planned time interval and incubated with DMMB and absorbance (TECAN infinite M200Pro, Switzerland) was determined at 595 nm (λ_{max}). Standard curve was determined from weighted amounts of GAGs in assessment aliquot. The GAGs release was assessed by Korsmeyer-Peppas [32] and Fick's law of diffusion [33–36] model.

2.6. Isolation and cultivation of cells

For *in vitro* studies, three different cells were used: human foreskin fibroblasts (Hs27; ATCC-CRL-1634; 19th passage), human mesenchymal stem cell (hMSCs; ethical no. EK 263122004; ethic vote No. EK 263122004) and human keratinocytes (HaCaT, Product Id. 300493, Cell Lines Service, Germany). Cultivation protocol and medium composition is described previously [20].

2.7. In vitro cell culture on electrospun scaffold

Scaffolds were cut into pieces with 10 mm diameter using a metallic punch and sterilized by UV treatment for 72 h. They were soaked into PBS and complete medium for 6 h and overnight at 37 °C, respectively. After removing medium, around 20,000 cells (in 80 μl medium) were seeded into each scaffold. Then the scaffolds were kept in CO_2 incubator for 2–3 h before adding medium to increase cellular adhesion efficiency. Culture medium was renewed thrice a week. Samples were collected for further biochemical (LDH and DNA quantification assay) evaluation when scaffold were 50% and 95% confluent with cells and stored at −80 °C until after washing with wash buffer. For immunofluorescence imaging, fixing was performed using 3.7% formaldehyde in PBS (Sigma) and stored at 4 °C.

2.8. Biochemical analysis

2.8.1. LDH assay

Thawed samples were treated with 1% Triton X-100 (Sigma Aldrich) PBS solution (Cell lysis buffer) for 50 min, followed by bath sonication

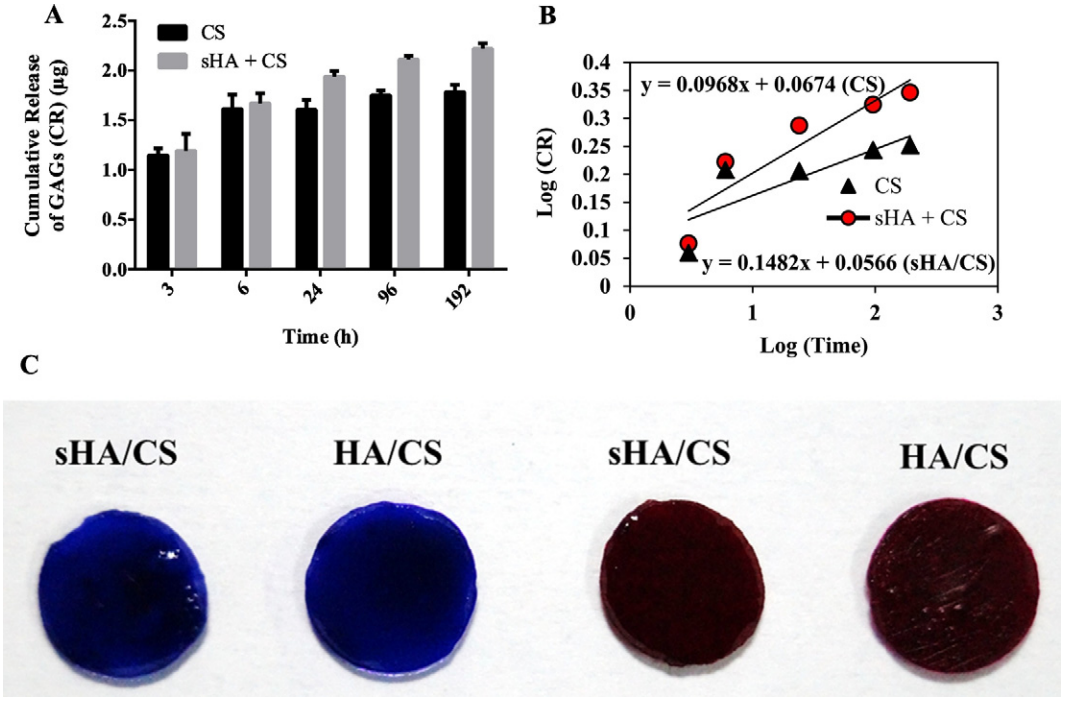

Fig. 2. Characterization of electrospun scaffolds; (A) release profile of sulfated GAGs from electrospun scaffolds as a function of time, (B) release kinetics as determined by DMMB assay. Distribution of GAGs and (C) Sirius red (right side: red color) and Toluidin blue (left side: blue color) staining of electrospun scaffold.

for 15 min. Lactate dehydrogenase (LDH) activity was evaluated by a Takara cytotoxicity detection kit (France) to determine the cellular growth. Concisely, 50 μl of cell lysate was mixed with 50 μl of LDH substrate for 4–6 min. Subsequently, 0.5 M HCl was added to each well to stop the enzymatic reaction. Finally, the absorbance was measured at 492 nm. Standard calibration curve was used to correlate the LDH activity of the samples.

2.8.2. DNA quantification

Cellular proliferation was measured by amount of DNA using PicoGreen assay kit (Thermo Fisher Scientific, USA). Cellular lysate per condition was incubated with Pico Green (lysate: Pico-Green = 1:19) in Tris EDTA buffer for 5 min. Fluorescence of the samples were measured spectroscopically (Ex- 485 nm, Em- 535 nm). Standard calibration curve was derived with DNA quantity of defined cell number. All experimental procedure was executed at room temperature.

2.8.3. Immunocytochemistry

Formaldehyde fixed samples were incubated with Triton™ X-100 (0.1%) in PBS for permeabilization followed by washing twice with wash buffer (0.05% (v/v) Tween-20 in PBS). Then the samples were incubated in 1% (w/v) BSA block solution for 30 min. Afterwards the samples were treated with Phalloidin 546 for 50 min. After washing, the samples were further incubated with DAPI (Thermo Fisher Scientific) for 5 min and again washed. Scaffolds were visualized on a fluorescence microscope equipped with 20 and 40 panfluor objectives (Carl Zeiss, Germany). All experimental procedure was executed at room temperature.

2.9. Statistical analysis

All studies have been performed in triplicate run and reported as mean ± standard deviation (SD). The statistical evaluation was performed by Two-way ANOVA and Bonferroni Post-hoc analysis (GraphPad Prism® 5) among two groups. p values are described as follows $^{*}p < 0.05$; $^{**}p < 0.01$; $^{***}p < 0.001$.

3. Results

3.1. Characterization of electrospun nanofibers

Fiber morphology of electrospun scaffold was analyzed by scanning electron microscopy (Fig. 1(A–D)). An evenly distributed fiber morphology was found with an average diameter of 260 ± 32 nm. No change in surface morphology of fibers was observed by varying concentrations

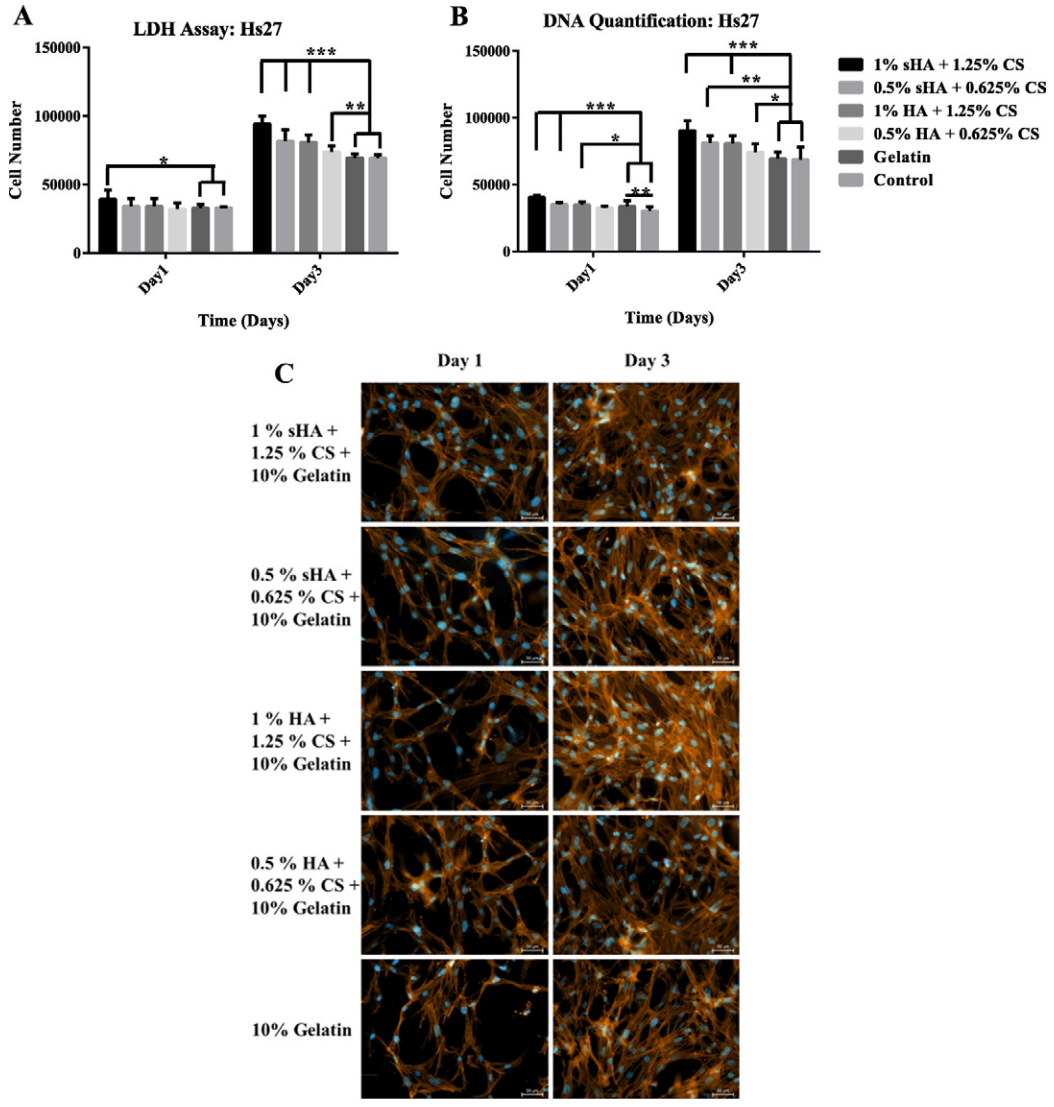

Fig. 3. Proliferation of fibroblasts (Hs27) was determined by LDH activity (A) and Pico Green dsDNA quantification (B). (C) Fibroblasts were cultured on scaffold and immunostained using Phalloidin (color: red-orange) and DAPI (Color: blue) for cytoskeleton and nucleus, respectively. For control, 10% gelatin scaffold was used. $^{*}p < 0.05$, $^{**}p < 0.01$, $^{***}p < 0.001$.

and types of GAGs. Fig. 1(E) shows the distribution of fiber diameters within the scaffolds.

The distribution of gelatin and GAGs (sHA and CS) was studied by Sirius red [28,29] and Toluidin blue [30] staining, respectively. Light microscope imaging revealed that the scaffolds were as fully stained red (gelatin) or blue (GAGs), which indicates even distribution of gelatin and GAGs throughout the scaffold (Fig. 2(C)).

The release of GAGs is shown in Fig. 2(A–B). Release coefficient value (n) of CS/sHA or CS/HA scaffold was observed as 0.1482 and 0.0968 as per Korsmeyer-Peppas model equation (Fickian diffusion: $n \leq 0.5$ and Non-Fickian diffusion: $0.5 < n \leq 1.0$), respectively. Hence, diffusion was the chief mechanism of GAGs release.

3.2. Cellular study on electrospun fibrous scaffolds

Initial attachment and growth rate of cells were examined on scaffolds with gelatin/CS/sHA or gelatin/CS/HA and collagen coated glass coverslip (as a control). Cellular attachment after 2 h of incubation in complete medium for Hs27 (14,980 ± 725), HaCaT (15,400 ± 832) and hMSCs (15,620 ± 628) was evaluated with LDH activity and DNA quantification. No significant difference in initial adhesion was observed while cultivating on electrospun scaffold with or without GAGs. Based on this finding all data were normalized for the initial adhesion cell number. Influence of GAGs (sHA/CS, HA/CS) on cellular proliferation was examined on electrospun scaffolds in terms of LDH activity and DNA content of cells (Figs. 3–5).

For all cells and scaffolds, similar proliferation behavior was observed for both LDH and DNA quantification assay. Hs27 (Fig. 3) and HaCaT (Fig. 4) doubled in number from day 1 to day 3. The same is true for hMSCs from day 7 to day 14 (Fig. 5). For all cell types scaffolds containing 1% sHA and 1.25% CS revealed the highest cell numbers at day 3 or day 14, respectively. In general, cellular number increased on scaffolds containing sulfated GAG components. This was dependent on sulfation degree (sHA *versus* HA) as well as concentration (1% *versus* 0.5% sHA or HA; 1.25% *versus* 0.625% CS).

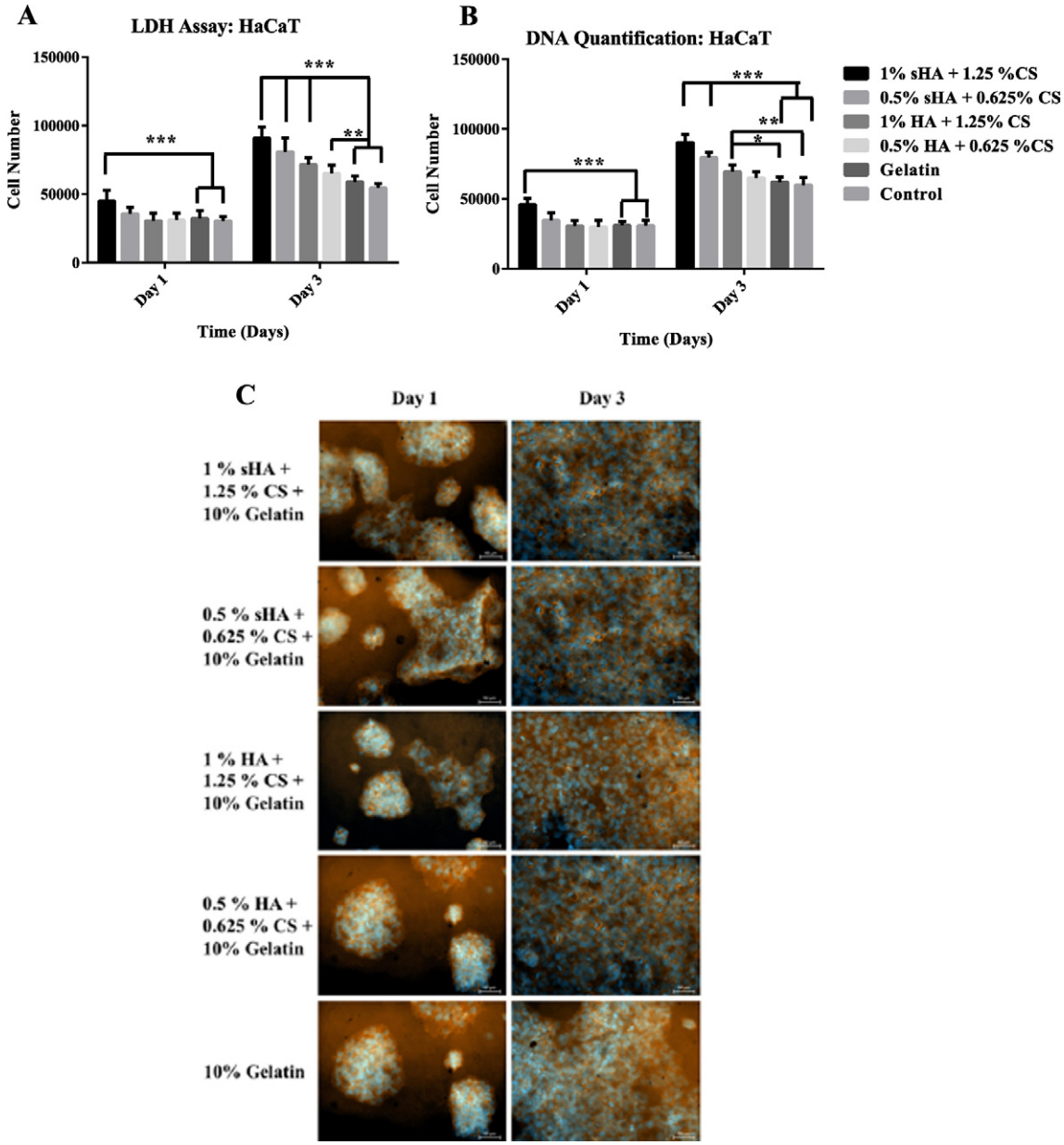

Fig. 4. Proliferation of keratinocytes (HaCaT) was determined by LDH activity (A) and Pico Green dsDNA quantification (B). (C) Keratinocytes were cultured on scaffold and immunostained using Phalloidin (color: red-orange) and DAPI (color: blue) for cytoskeleton and nucleus, respectively. For control, 10% gelatin scaffold was used. $^{*}p < 0.05$, $^{**}p < 0.01$, $^{***}p < 0.001$.

Cellular behavior on electrospun scaffolds was further assessed microscopically by immunostaining cytoskeleton and nucleus with Phalloidin and DAPI, respectively. Under our conditions, Hs27 (Fig. 3), HaCaT (Fig. 4) and hMSCs (Fig. 5) adhered, proliferated on all substrates investigated. Cells were firmly adhered to the nanofibers and stretched very well along the scaffolds. As shown in Figs. 3–5, scaffolds with GAGs showed relatively higher cell viability in comparison with simple gelatin nanofibrous scaffold for all three cell types. Increase in cellular proliferation was observed with increasing concentration of GAGs for all three cell types by analyzing the images. However, cell growth on nanofibrous scaffold with sulfated GAGs (sHA and CS) was obviously higher than that of nanofibrous scaffold with or without native GAGs (HA and CS) for all three cell types. Finding of immunofluorescence imaging supports the results of LDH and DNA quantification assay in earlier section. The qualitative analysis supported the quantitative findings in terms of increased cell numbers over time and an enhanced proliferation depending on sulfation degree and GAG concentration (Figs. 3–5). These results indicated that nanofibrous scaffold releasing GAGs in a sustainable manner to promote cellular proliferation.

4. Discussion

The primary function of biomaterials is to provide a platform for the injured tissue and support wound healing processes [37]. Material-tissue interaction is generally mediated by specific cell surface receptors. Therefore, primary role of the biomaterial is to provide an appropriate stage for cellular attachment, growth and differentiation. Against this background, this study aims to develop defined functional cellular microenvironments created by biomimetic electrospun scaffolds from main extracellular matrix components (gelatin, CS and sHA or HA), which are supposed to mimic the native ECM of dermal tissue.

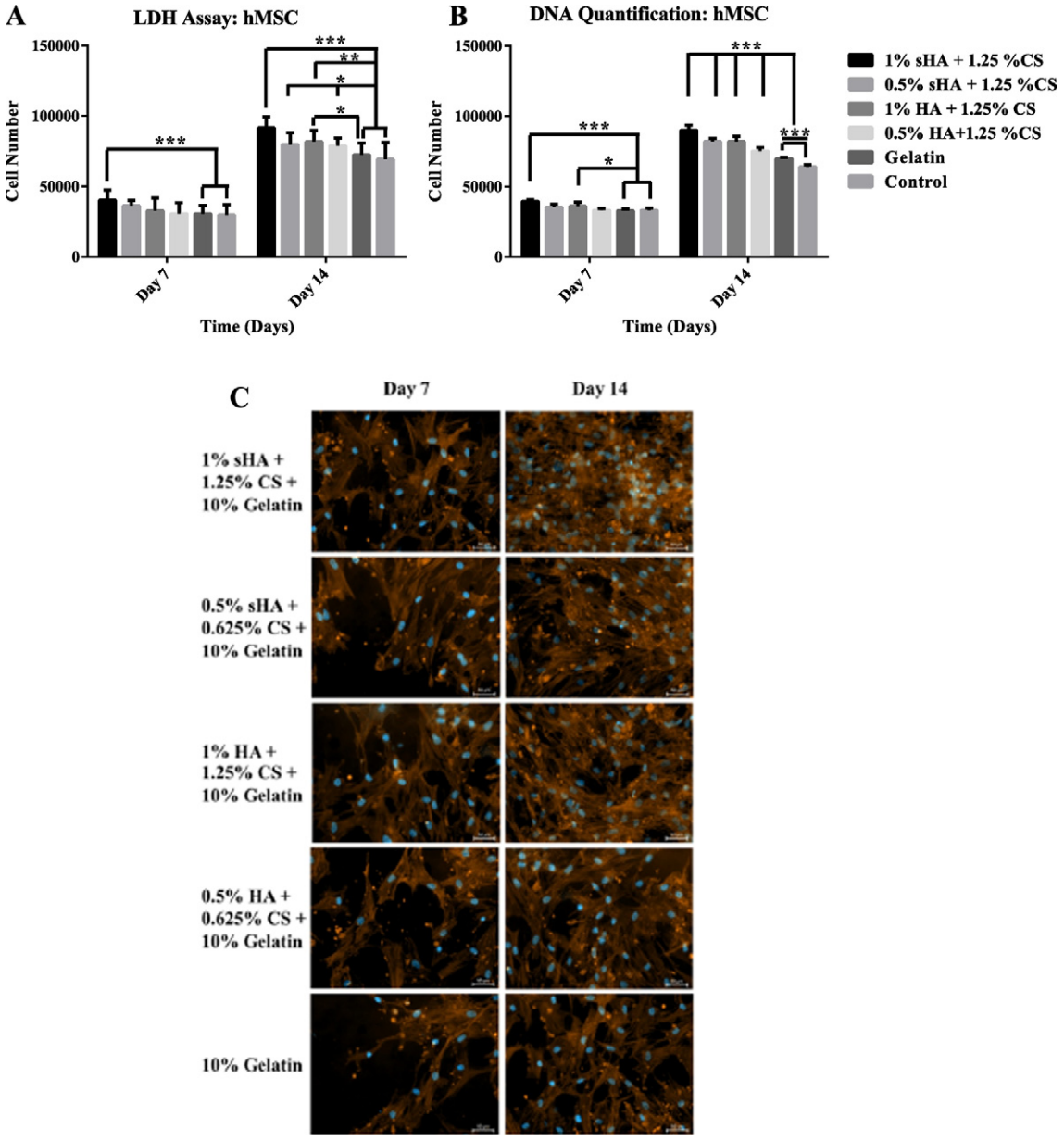

Fig. 5. Proliferation of hMSCs, as determined by LDH activity (A) and Pico Green dsDNA quantification (B). (C) hMSCs were cultured on scaffold and immunostained using Phalloidin (Color: red-orange) and DAPI (Color: blue) for cytoskeleton and nucleus, respectively. For control, 10% gelatin scaffold was used. $^{*}p < 0.05$, $^{**}p < 0.01$, $^{***}p < 0.001$.

4.1. Morphology and characterization of tri-copolymer electrospun scaffold

Evenly distributed fiber morphology was observed (Fig. 1(A–E)), independent from the presence of different GAG concentrations, GAGs backbone and degree of sulfation. Li et al. likewise did not observe any difference in fiber diameter and shape by varying HA concentrations while electrospinning gelatin-HA blend solution [38].

The *in vitro* release kinetics of GAGs from electrospun scaffold revealed Fickian diffusion (Fig. 2(A–B)). Slow and sustained GAGs release was observed from electrospun scaffold because they were crosslinked with GTA vapor. Electrostatic interactions between gelatin [39] (cationic in nature) and GAGs [40] (anionic in nature) may be responsible for this. However, because of hydrophilic nature of sulfated GAGs (sHA/CS), higher release behavior (2.21 ± 0.05 μg/ml in 192 h) was observed here compared to our previous work where GAGs (CS) release was 1.92 ± 0.05 μg/ml in 192 h [20].

4.2. Effects of tri-copolymer electrospun scaffold on cells

Electrospun scaffold (with or without GAGs) assisted Hs27, HaCaT and hMSCs' attachment to the scaffold after 2 h. Around 75% initial adhesion was observed for all cell types independent of scaffold type. The RGD motives of gelatin may support cellular attachment to the scaffold surface [41]. However, no significant differences were observed among different scaffold types. In contrast, van der Smissen et al. demonstrated that high sulfation of GAGs promote the initial cellular attachment of human dermal fibroblasts on 2D aECM scaffold comprised of sulfated hyaluronan and collagen I within 1 h [1]. One reason for this deviating result might be that GAGs composition and concentration are presented differently in 2D matrices and 3D electrospun scaffolds.

Proliferation and migration of fibroblasts and keratinocytes play a fundamental role in early stages of dermal wound healing [42,43]. Significant cellular growth was observed after cultivating the cells in the electrospun scaffold with sHA and CS for longer time periods using LDH activity and DNA content of cells (Figs. 3–5). Those scaffolds consisting of 1% sHA and 1.25% CS revealed a higher proliferation than scaffold consisting of non-sulfated 1% HA and 1.25% CS for all three cell type. This is in line with outcomes of van der Smissen et al. demonstrating an increased proliferation on collagen I/sulfated glycosaminoglycans containing scaffolds for human dermal fibroblasts [1]. They showed that degree of sulfation of GAGs influence cell proliferation in a progressive manner in human dermal fibroblasts [1]. Franz et al. showed that sulfated GAGs (sHA, CS) influence cellular behavior in a positive manner compared to non-sulfated GAGs in human pro-inflammatory M1 macrophages [21,44]. Comparing the two types of scaffold used in this study, we believe that one possible reason for this set of results might be the structural differences between sulfated HA and native HA. As described in the introduction section, except for hyaluronan most of the native GAGs are sulfated and negatively charged linear polysaccharides [5,45]. Considering the average degree of sulfation, sulfated HA ($DS_S \sim 3$) can represent a highly sulfated GAG like heparan sulfate. Unlike native HA, the primary OH group of the *N*-acetylglucosamine sugar unit of sulfated HA (C-6 position) is completely sulfated and the secondary OH located at C-2, C-3 and C-4 position of equatorial one are partly sulfated [21]. Hintze et al. showed that the differences in the degree of sulfation as well as the sulfation pattern can alter the binding affinities for several growth factors [21,46]. This higher growth factors binding affinity of sHA might promote the availability of active, stabilized growth factors, cations such as Ca^{2+} ions and therefore stimulate cellular behavior. Besides the microenvironment, cell-cell contacts play an important role in cellular signaling required for cellular proliferation during wound healing process [47,48]. All three cell types showed significantly higher proliferation on the highly sulfated GAGs containing scaffold compared to native non-sulfated GAGs containing scaffold.

Based on the observed *in vitro* studies of electrospun scaffolds composed of sulfated GAGs on fibroblasts (Hs27), keratinocytes (HaCaT) and hMSCs an accelerated start for the process of the wound healing due to improved cellular proliferation and migration can be expected.

5. Conclusion

The aim of this study was to develop biomimetic electrospun scaffolds from main extracellular matrix components to be used as biofunctional dermal wound dressing materials promoting epidermal-dermal healing processes. Those nanofibrous scaffolds containing chemically sulfated GAGs enhanced fibroblast, keratinocyte and hMSCs proliferation. Therefore this study implies that highly sulfated GAG containing electrospun nanofibrous scaffolds might lead to effective skin tissue engineered constructs enhancing cellular performance and therefore foster epidermal-dermal wound healing.

Notes

The authors declare no competing financial interest.

Acknowledgments

The authors are grateful for the financial assistantship provided by DFG, TRR 67 (A2, A3, Z3) and DAAD, Germany. Authors would also like to acknowledge Mr. Ronny Bruenler, group of Prof. Chokri Cherif, Institute of Textile Machinery and High Performance Material Technology, TU Dresden, Germany for providing the electrospinning facility and Rene Beutner, Erik Wegener and Lucas Schirmer for their assistance.

References

[1] A. van der Smissen, V. Hintze, D. Scharnweber, S. Moeller, M. Schnabelrauch, A. Majok, J.C. Simon, U. Anderegg, Biomaterials 32 (2011) 8938–8946.
[2] M. Nagahata, T. Tsuchiya, T. Ishiguro, N. Matsuda, Y. Nakatsuchi, A. Teramoto, A. Hachimori, K. Abe, Biochem. Biophys. Res. Commun. 315 (2004) 603–611.
[3] Y. Kang, S. Kim, A. Khademhosseini, Y. Yang, Biomaterials 32 (2011) 6119–6130.
[4] B.-H. Choi, Y.S. Choi, D.G. Kang, B.J. Kim, Y.H. Song, H.J. Cha, Biomaterials 31 (2010) 8980–8988.
[5] K.J. Manton, L.M. Haupt, K. Vengadasalam, V. Nurcombe, S.M. Cool, J. Mol. Histol. 38 (2007) 415–424.
[6] C.-H. Chang, H.-C. Liu, C.-C. Lin, C.-H. Chou, F.-H. Lin, Biomaterials 24 (2003) 4853–4858.
[7] C.I. Gama, S.E. Tully, N. Sotogaku, P.M. Clark, M. Rawat, N. Vaidehi, W.A. Goddard, A. Nishi, L.C. Hsieh-Wilson, Nat. Chem. Biol. 2 (2006) 467–473.
[8] T.W. Wang, H.C. Wu, Y.C. Huang, J.S. Sun, F.H. Lin, Artif. Organs 30 (2006) 141–149.
[9] W. Wang, M. Zhang, W. Lu, X. Zhang, D. Ma, X. Rong, C. Yu, Y. Jin, Tissue Eng. Part C Methods 16 (2009) 269–279.
[10] S. Yan, Q. Zhang, J. Wang, Y. Liu, S. Lu, M. Li, D.L. Kaplan, Acta Biomater. 9 (2013) 6771–6782.
[11] T.-W. Wang, J.-S. Sun, H.-C. Wu, Y.-H. Tsuang, W.-H. Wang, F.-H. Lin, Biomaterials 27 (2006) 5689–5697.
[12] N. Sawatjui, T. Damrongrungruang, W. Leeanansaksiri, P. Jearanaikoon, T. Limpaiboon, Mater. Lett. 126 (2014) 207–210.
[13] V. Koul, S. Bhowmick, A.V. Thanusha, Hydrogels for Pharmaceutical Applications, Handbook of Polymers for Pharmaceutical Technologies, John Wiley & Sons, Inc., 2015 125–144.
[14] D. Kai, M.P. Prabhakaran, B.Q.Y. Chan, S.S. Liow, S. Ramakrishna, F. Xu, X.J. Loh, Biomed. Mater. 11 (2016), 015007.
[15] J. Hu, D. Kai, H. Ye, L. Tian, X. Ding, S. Ramakrishna, X.J. Loh, Mater. Sci. Eng. C 70 (2017) 1089–1094.
[16] D. Kai, S.S. Liow, X.J. Loh, Mater. Sci. Eng. C 45 (2014) 659–670.
[17] D. Kai, M.J. Tan, M.P. Prabhakaran, B.Q.Y. Chan, S.S. Liow, S. Ramakrishna, X.J. Loh, Colloids Surf. B: Biointerfaces 148 (2016) 557–565.
[18] R. Lakshminarayanan, R. Sridhar, X.J. Loh, M. Nandhakumar, V.A. Barathi, M. Kalaipriya, J.L. Kwan, S.P. Liu, R.W. Beuerman, S. Ramakrishna, Int. J. Nanomedicine 9 (2014) 2439.
[19] X.J. Loh, P. Peh, S. Liao, C. Sng, J. Li, J. Control. Release 143 (2010) 175–182.
[20] S. Bhowmick, D. Scharnweber, V. Koul, Biomaterials 88 (2016) 83–96.
[21] V. Hintze, S. Moeller, M. Schnabelrauch, S. Bierbaum, M. Viola, H. Worch, D. Scharnweber, Biomacromolecules 10 (2009) 3290–3297.
[22] J. Salbach-Hirsch, J. Kraemer, M. Rauner, S.A. Samsonov, M.T. Pisabarro, S. Moeller, M. Schnabelrauch, D. Scharnweber, L.C. Hofbauer, V. Hintze, Biomaterials 34 (2013) 7653–7661.
[23] R. Kunze, M. Rösler, S. Möller, M. Schnabelrauch, T. Riemer, U. Hempel, P. Dieter, Glycoconj. J. 27 (2010) 151–158.
[24] S. Rother, J. Salbach-Hirsch, S. Moeller, T. Seemann, M. Schnabelrauch, L.C. Hofbauer, V. Hintze, D. Scharnweber, ACS Appl. Mater. Interfaces (2015) 23787–23797.

[25] Y. Zhang, J. Venugopal, Z.-M. Huang, C. Lim, S. Ramakrishna, Polymer 47 (2006) 2911–2917.
[26] S. Bhowmick, D.K. Das, A.K. Maiti, C. Chakraborty, Micron 44 (2013) 384–394.
[27] S. Bhowmick, D.K. Das, A.K. Maiti, C. Chakraborty, J. Med. Imaging Health Inform. 2 (2012) 215–221.
[28] L.A. Condezo-Hoyos, G. Espana-Caparros, A.L.L. de Pablo, P. Rodriguez-Rodriguez, P.Y. Gutierrez-Arzapalo, J. Ancer, M.C. Gonzalez, S.M. Arribas, FASEB J. 26 (2012) lb201.
[29] F. Prins, I. Velde, E. de Heer, Humana Press Totowa, NJ, 2006, 363–401.
[30] D. Terry, R. Chopra, J. Ovenden, T. Anastassiades, Anal. Biochem. 285 (2000) 211–219.
[31] R.W. Farndale, D.J. Buttle, A.J. Barrett, Biochim. Biophys. Acta Gen. Subj. 883 (1986) 173–177.
[32] R.W. Korsmeyer, R. Gurny, E. Doelker, P. Buri, N.A. Peppas, Int. J. Pharm. 15 (1983) 25–35.
[33] P.L. Ritger, N.A. Peppas, J. Control. Release 5 (1987) 37–42.
[34] M. Jaiswal, A.K. Dinda, A. Gupta, V. Koul, Biomed. Mater. 5 (2010), 065014.
[35] S. Bhowmick, V. Koul, Mater. Sci. Eng. C 59 (2016) 109–119.
[36] S. Bhowmick, S. Mohanty, V. Koul, J. Mater. Sci. Mater. Med. 27 (2016) 1–12.
[37] D.F. Williams, Biomaterials 30 (2009) 5897–5909.
[38] J. Li, A. He, C.C. Han, D. Fang, B.S. Hsiao, B. Chu, Macromol. Rapid Commun. 27 (2006) 114–120.
[39] P. Dubruel, Cationic Polymers in Regenerative Medicine, Royal Society of Chemistry, 2014.
[40] C.J. Taylor, R.M. Burke, B. Wu, S. Panja, S.B. Nielsen, C.E. Dessent, Int. J. Mass Spectrom. 285 (2009) 70–77.
[41] E. Ruoslahti, Annu. Rev. Cell Dev. Biol. 12 (1996) 697–715.
[42] A.D. Metcalfe, M.W. Ferguson, J. R. Soc. Interface 4 (2007) 413–437.
[43] A.D. Metcalfe, M.W. Ferguson, Biomaterials 28 (2007) 5100–5113.
[44] S. Franz, F. Allenstein, J. Kajahn, I. Forstreuter, V. Hintze, S. Möller, J.C. Simon, Acta Biomater. 9 (2013) 5621–5629.
[45] M. Büttner, S. Möller, M. Keller, D. Huster, J. Schiller, M. Schnabelrauch, P. Dieter, U. Hempel, J. Cell. Physiol. 228 (2013) 330–340.
[46] V. Hintze, A. Miron, S. Moeller, M. Schnabelrauch, H.-P. Wiesmann, H. Worch, D. Scharnweber, Acta Biomater. 8 (2012) 2144–2152.
[47] M.F. Pittenger, A.M. Mackay, S.C. Beck, R.K. Jaiswal, R. Douglas, J.D. Mosca, M.A. Moorman, D.W. Simonetti, S. Craig, D.R. Marshak, Science 284 (1999) 143–147.
[48] D.J. Prockop, Science 276 (1997) 71–74.